

Abstract

We examine CMIP6 simulations of Arctic sea-ice area and volume. We find that CMIP6 models produce a wide spread of mean Arctic sea-ice area, capturing the observational estimate within the multi-model ensemble spread. The CMIP6 multi-model ensemble mean provides a more realistic estimate of the sensitivity of September Arctic sea-ice area to a given amount of anthropogenic CO₂ emissions and to a given amount of global warming, compared with earlier CMIP experiments. Still, most CMIP6 models fail to simulate at the same time a plausible evolution of sea-ice area and of global mean surface temperature. In the vast majority of the available CMIP6 simulations, the Arctic Ocean becomes practically sea-ice free (sea-ice area < 1 million km²) in September for the first time before the year 2050 in each of the four emission scenarios SSP1-1.9, SSP1-2.6, SSP2-4.5 and SSP5-8.5 examined here.

Plain Language Summary

We examine simulations of Arctic sea ice from the latest generation of global climate models. We find that the observed evolution of Arctic sea-ice area lies within the spread of model simulations. In particular, the latest generation of models performs better than models from previous generations at simulating the sea-ice loss for a given amount of CO₂ emissions and for a given amount of global warming. In most simulations, the Arctic Ocean becomes practically sea-ice free (sea-ice area < 1 million km²) in September for the first time before the year 2050.

1 Introduction

In recent decades, Arctic sea-ice area has decreased rapidly, and the signal of a forced sea-ice retreat has clearly emerged from the background noise of year-to-year variability. Because of this, the ability of climate models to plausibly simulate the observed changes in Arctic sea-ice coverage has become a central measure of model performance in Arctic-focused climate model intercomparisons (e.g., Koenig et al., 2014; Massonnet et al., 2012; Melia et al., 2015; Olonscheck & Notz, 2017; Shu et al., 2015; Stroeve et al., 2007, 2012, 2014). In this contribution, we extend these earlier studies that examined model performance in the third and fifth phases of the Coupled Model Intercomparison Project (CMIP3 and CMIP5) by examining model simulations from the sixth phase of the Coupled Model Intercomparison Project (CMIP6, Eyring et al., 2015). For CMIP6, the Sea-Ice Model

50 Intercomparison Project (SIMIP, Notz et al., 2016) designed a specific set of diagnos-
51 tics that allow for detailed analyses of sea-ice related processes and thus a process-based
52 evaluation of sea-ice simulations of the participating models. To lay the foundation for
53 such analyses, we here provide an initial overview of CMIP6 model performance by ex-
54 amining some large-scale, pan-Arctic metrics of model performance and future sea-ice
55 evolution, including a comparison to CMIP5 and CMIP3 simulations. A similar anal-
56 ysis for Antarctic sea ice is given by (Roach et al., under review).

57 2 Analysis Method

58 In this contribution, we examine two large-scale integrated quantities that describe
59 the time evolution of Arctic sea ice. These are the Northern Hemisphere total sea-ice area
60 (SIA) and total sea-ice volume (SIV), which can be calculated readily from SIMIP vari-
61 ables as follows.

62 To obtain sea-ice area for CMIP6 model simulations, we use the SIMIP variable
63 of Northern Hemisphere sea-ice area `siarean` when provided. If `siarean` is not provided,
64 we calculate the sea-ice area by multiplying sea-ice concentration on the ocean grid (`siconc`,
65 preferred) or on the atmospheric grid (`siconca`) with individual grid-cell area and then
66 sum over the Northern Hemisphere. Note that we use sea-ice area as our primary vari-
67 able to describe sea-ice coverage instead of sea-ice extent, which is usually calculated as
68 the total area of all grid cells with at least 15% sea-ice concentration. Our choice to fo-
69 cus on sea-ice area derives primarily from the fact that sea-ice extent is a strongly grid-
70 dependent, non-linear quantity, making it difficult to meaningfully compare between model
71 output and satellite observations (compare Notz, 2014). In addition, the observational
72 spread across different satellite products is smaller for trends in sea-ice area than it is
73 for trends in sea-ice extent (Comiso et al., 2017).

74 To calculate sea-ice volume for CMIP6 models, we (1) directly use the SIMIP vari-
75 able of Northern Hemisphere sea-ice volume `sivoln` when provided, or (2) multiply the
76 sea-ice volume per grid-cell area `sivo1` by individual grid-cell area and sum over the North-
77 ern Hemisphere, or (3) multiply sea-ice-concentration `siconc`, sea-ice thickness `sithick`
78 and individual grid-cell area and then sum over the Northern Hemisphere. For CMIP5,
79 only the sea-ice volume per grid-cell area (also called “equivalent sea-ice thickness”, `sit`)
80 is available, so we use method (2) for all CMIP5 models. We were unable to obtain sea-

81 ice volume data for CMIP3 models, so volume comparisons in the following are limited
82 to CMIP5 and CMIP6 model simulations.

83 To meaningfully estimate model performance relative to the real evolution of the
84 sea-ice cover in the Arctic, we must take internal variability into account (see, for ex-
85 ample, England et al., 2019; Kay et al., 2011; Notz, 2015; Olonscheck & Notz, 2017; Swart
86 et al., 2015). Internal variability describes the spread in plausible climate trajectories
87 in response to a given forcing scenario, owing to the chaotic nature of our climate sys-
88 tem. The observational record is just one such plausible trajectory, and no single model
89 simulation can ever be expected to perfectly agree with it because of its chaotic nature.
90 Therefore, most CMIP6 models have been run several times with slightly different ini-
91 tial conditions to estimate the range of trajectories that are compatible with a given model's
92 physics. In the following, we take two different approaches to examine whether a given
93 model provides a plausible simulation of the observational record in light of internal vari-
94 ability.

95 First, for CMIP6 models, we estimate a best-guess CMIP6-average internal vari-
96 ability σ_{cmip6} by averaging across the individual ensemble spread of those models that
97 provide three or more ensemble members (see Table S3 for details). In calculating the
98 standard deviation, we correct for small sample size n by using Bessel's correction and
99 then dividing the resulting standard deviation by the scale mean of the chi distribution
100 with $n-1$ degrees of freedom. We then define all simulations that lie within the range
101 of $2\sigma = \pm 2\sqrt{\sigma_{cmip6}^2 + \sigma_{obs}^2}$ around the observational estimate as plausible simulations
102 (compare Olonscheck & Notz, 2017). Here, σ_{obs}^2 refers to the observational uncertainty
103 explained below. This approach allows us to also examine the plausibility of those mod-
104 els that only provide a single ensemble member. In addition to considering internal vari-
105 ability explicitly, we reduce its impact by examining model performance relative to a time
106 average over several years. We take the first twenty years of the satellite record (1979–
107 1998) for comparing mean values, as those twenty years provide a compromise between
108 using as many years as possible and using a period with no strong trend in Arctic sea-
109 ice area and volume. However, even on multi-decadal time scales internal variability af-
110 fects the Arctic sea-ice cover, so averaging over 20 years is not long enough an averag-
111 ing period to remove the impact of internal variability entirely. To compare trends, we
112 examine the overlap period 1979–2014 of the satellite record, which begins in 1979, and
113 the historical period of CMIP6, which ends in 2014.

114 Second, in order to select a subset of models for estimating a best guess of the fu-
115 ture evolution of the Arctic sea-ice cover, we take the more strict approach to define a
116 model as plausible if its ensemble spread includes the observational record, considering
117 observational uncertainty. These models are referred to as “selected models” hereafter.

118 To obtain an observational estimate of sea-ice area, we use observational records
119 of sea-ice concentration from the OSI SAF (Lavergne et al., 2019), NASA-Team (Cavalieri
120 et al., 1997) and Bootstrap (Comiso et al., 1997) algorithms. Sea-ice area is then cal-
121 culated by multiplying the sea-ice concentration with individual grid-cell area and sum-
122 ming over the Northern Hemisphere. For the NASA-Team and Bootstrap algorithms,
123 we filled the observational pole hole with the average sea-ice concentration around its
124 edge (Olason & Notz, 2014). For OSI SAF, we used the filled pole hole of the product
125 itself. We take the spread of the three algorithms obtained this way as the observational
126 uncertainty σ_{obs} .

127 For sea-ice volume, we do not compare models with an observational estimate due
128 to substantial uncertainties for reanalysed and observed estimates of Arctic sea-ice thick-
129 ness and thus volume (e.g. Bunzel et al., 2018; Chevallier et al., 2017; Zygmontowska
130 et al., 2014).

131 For global-mean surface temperature (GMST), we use the average of NOAA Glob-
132 alTemp v5.0.0 (Vose et al., 2012), GISTemp v4 (GISTEMP Team, 2019; Lenssen et al.,
133 2019), HadCRUT4.6.0.0 (Morice et al., 2012) and Berkeley (Rohde et al., 2013) time-
134 series as an estimate for the mean evolution, and the spread across these four records
135 as an estimate for observational uncertainty. We calculate anomalies relative to the pe-
136 riod 1850–1900, except for the shorter record of NOAA GlobalTemp where we calculate
137 anomalies relative to 1880–1900. Because the 20-year running-mean temperature fluc-
138 tuations during these periods are less than 0.1 °C, our results are largely insensitive to
139 this choice of baseline period (Figure S2). We take the spread of the four products as
140 the observational uncertainty σ_{obs} .

141 Historical anthropogenic CO₂ emissions are taken from the historical budget of (Global
142 Carbon Project, 2019). Future anthropogenic CO₂ emissions for CMIP6 simulations are
143 taken from the respective SSP scenarios described by (Riahi et al., 2017).

3 CMIP6 Model Performance

3.1 Mean Quantities

We start with an analysis of the mean sea-ice fields simulated by individual CMIP3, CMIP5 and CMIP6 models (Figure 1a, b, e, f) over the period 1979–1998. To allow for a fair comparison across the three CMIP phases, in this section we analyze only the first ensemble member of each model. Given the large number of participating models, this results in a fair comparison: for models with several ensemble members, the first ensemble member is as likely to be above a model’s ensemble mean as below.

For sea-ice area, we find a large spread across CMIP6 simulations both in March and in September (Figure 1a, b), which usually are the months of maximum and minimum sea-ice coverage in the Arctic, respectively. In March, the 1979–1998 mean sea-ice area simulated by CMIP6 models ranges from around 12 million km² to more than 20 million km² and thus includes the observational estimate of 14.4 million km² (Figure 1a, Table S3). Out of the 40 CMIP6 models, 21 are within the $2\sigma = \pm 1.29$ million km² plausibility range around the observational estimate given by the CMIP6-average internal variability and observational uncertainty as introduced in section 2 (Figure 1a, Table S3). CMIP3 and CMIP5 simulations also show a large spread in mean March sea-ice area, and include the observational estimate within their multi-model ensemble spread (Figure 1a, Tables S1 and S2). However, in CMIP3 and CMIP5, the multi-model ensemble spread is more evenly distributed around the observational estimate than in CMIP6, where most models lie above it.

For the mean September sea-ice area over the period 1979–1998, the CMIP6 ensemble also shows a large spread of individual simulations, ranging from around 3 million km² to around 10 million km² (Figure 1b, Table S3). The observed value of around 6 million km² lies well within the range, and 25 out of 40 CMIP6 models are within the plausible range of $2\sigma = \pm 1.49$ million km² around this value (Table S3). The CMIP6 multi-model ensemble mean is very close to the observational estimate and well within the plausible range. The same holds for CMIP3 and CMIP5, with their individual models also spanning a wide range around the observational estimate (Figure 1b, Tables S1 and S2).

174 For sea-ice volume, we lack data for CMIP3 models and thus can only compare CMIP6
175 results to CMIP5 results (see tables S2 and S3 for a detailed overview). For both phases
176 of CMIP, the models produce a similar spread of simulated Arctic sea-ice volume from
177 less than 20,000 km³ to more than 40,000 km³ in March (Figure 1e), and from less than
178 5,000 km³ to more than 30,000 km³ in September (Figure 1f). Given a simulated aver-
179 age spread from internal variability of around 2,000 km³, the large spread in sea ice vol-
180 ume from CMIP6 models can not be explained by internal variability alone. Instead, it
181 is caused by the models' large spread in simulated sea-ice area and thickness.

182 Based on this analysis of mean Arctic sea-ice quantities, we find that there is lit-
183 tle difference in overall model performance between CMIP3, CMIP5 and CMIP6. The
184 multi-model spread of the mean quantities remains large, the observational record lies
185 within the multi-model ensemble spread, and many models simulate plausible values of
186 mean sea-ice area when considering the impact of internal variability and observational
187 uncertainty. The multi-model ensemble means of the past three phases of CMIP are rel-
188 atively similar to each other and largely consistent with the observational record.

189 3.2 Sensitivity

190 In addition to their plausible simulation of mean quantities, the models' adequacy
191 for simulating reality hinges critically on their ability to realistically simulate the response
192 of a given climate metric to changes in external forcing. Internal variability causes a large
193 spread of plausible climate trajectories in response to a given change in the forcing and
194 must carefully be taken into account when interpreting a possible mismatch between a
195 simulation and a given observational sea-ice record (Jahn et al., 2016; Kay et al., 2011;
196 Notz, 2015; Olonscheck & Notz, 2017; Swart et al., 2015). We find this to remain valid
197 for CMIP6 simulations.

198 For our analysis of the simulated sensitivity of Arctic sea ice to changes in exter-
199 nal forcing, we calculate two distinct quantities: first, the change in sea-ice area for a given
200 change in cumulative anthropogenic CO₂ emissions over the period 1979–2014 (Figure
201 1c); second, the change in sea-ice area for a given change in global mean surface tem-
202 perature (GMST) over the period 1979–2014 (Figure 1d). Both quantities can be cal-
203 culated from the previously demonstrated linear relationships of sea-ice area to cumu-
204 lative CO₂ emissions (Herrington & Zickfeld, 2014; Notz & Stroeve, 2016; Zickfeld et al.,

205 2012) and to GMST (e.g., Gregory et al., 2002; Mahlstein & Knutti, 2012; Rosenblum
206 & Eisenman, 2016; Stroeve & Notz, 2015; Winton, 2011). Together, these two quanti-
207 ties allow us to estimate whether CMIP6 models simulate changes in sea ice with the cor-
208 rect sensitivity to changes in external forcing, and whether they potentially do so for the
209 right reason. This is because the relationship between sea-ice area and cumulative an-
210 thropogenic CO₂ emissions is an almost linear proxy for the long-term time evolution
211 of Arctic sea-ice area, as cumulative emissions map monotonously to time. In contrast,
212 the sensitivity of sea-ice area to GMST changes is a proxy for the sensitivity of the sea-
213 ice cover to one particular response of the climate system to changes in external forc-
214 ing.

215 Our analysis reveals that over the historical period 1979–2014, 28 out of 40 CMIP6
216 models simulate a sensitivity of the Arctic sea-ice area to cumulative anthropogenic CO₂
217 emissions that is within the plausible range of 2.73 ± 1.37 m² of sea-ice loss per ton of CO₂
218 emissions (Figure 1c, Table S3). In addition to the larger spread of the CMIP6 multi-
219 model ensemble, a major difference between CMIP5 and CMIP6 models is that, in their
220 first ensemble member analyzed here, only 3 out of 40 CMIP5 models simulate a larger
221 loss of sea-ice area per ton of CO₂ emissions than observed. This number increases to
222 10 out of 40 models for CMIP6. This results in the CMIP6 multi-model ensemble mean
223 being closer to the observational estimate than the CMIP5 and the CMIP3 multi-model
224 ensemble means. It is however unclear whether this reflects an improvement of model
225 physics or primarily arises from the change in historical forcing in CMIP6 relative to CMIP5
226 (compare Rosenblum & Eisenman, 2016). For example, in CMIP6 the historical ozone
227 radiative forcing is about 80 % higher than it was in CMIP5 (Checa-Garcia et al., 2018).
228 In contrast, black carbon emissions in the CMIP6 historical forcing are substantially higher
229 over the past years than prescribed in the CMIP5 RCP8.5 scenario (Gidden et al., 2019).
230 The impact of these changes in non-CO₂ climate drivers is confounded into the sensi-
231 tivity of sea-ice area to CO₂ emissions (again, compare Rosenblum & Eisenman, 2016).
232 Emissions of CO₂ itself, and of methane, are largely unchanged over the historical pe-
233 riod for CMIP5 and CMIP6. However, for the future simulations the CMIP6 SSP5-8.5
234 scenario assumes higher CO₂ emissions and lower methane emissions than the CMIP5
235 RCP8.5 scenario (Gidden et al., 2019).

236 Examining the sea-ice loss per degree of global warming, we find that only 11 out
237 of 40 CMIP6 models are within the plausible range of 4.01 ± 1.28 million m² of sea-ice

238 loss per degree of warming (Figure 1d, Table S3). This is comparable to CMIP5, where
239 9 out of 40 models were within this plausible range (Figure 1d, Table S2). In CMIP3,
240 not a single model provided a plausible sensitivity (Figure 1d). Also, the CMIP6 multi-
241 model ensemble mean of Arctic sea-ice loss for a given amount of global warming is closer
242 to (but still outside) the plausible range than the multi-model ensemble mean of both
243 CMIP5 and CMIP3. This might indicate an improvement of CMIP6 models over pre-
244 vious CMIP phases on a process level, given that the main physical link of sea-ice loss
245 to any change in external forcing is given by a change in temperature. However, as be-
246 fore, this might also be a reflection of a more realistic historical forcing of CMIP6 com-
247 pared to CMIP5 and CMIP3.

248 While the more realistic simulation of these two sensitivities might indicate progress
249 in CMIP6 models' capability to simulate the ongoing loss of Arctic sea ice, as in CMIP5
250 (Rosenblum & Eisenman, 2017) few CMIP6 models are able to simulate a plausible amount
251 of sea-ice loss and simultaneously a plausible change in global mean temperature over
252 time (or cumulative anthropogenic CO₂ emissions). Of the CMIP6 models analyzed here,
253 these are ACCESS-CM2, BCC-CSM2-MR, CNRM-CM6-1-HR, FGOALS-f3-L, FIO-ESM-
254 2-0, GFDL-ESM4, GISS-E2-1-G, GISS-E2-1-G-CC, MPI-ESM-1-2-HAM, MPI-ESM1-
255 2-HR, MPI-ESM1-2-LR, MRI-ESM2-0 and NorESM2-MM. For the other CMIP6 mod-
256 els, those models that have a reasonable sea-ice loss tend to have too much global warm-
257 ing, while those models that simulate reasonable global warming simulate too little sea-
258 ice loss (Figure 1g, Table S3). In particular, the models with a high sensitivity of Arc-
259 tic sea-ice area to anthropogenic CO₂ emissions also display a high sensitivity of global
260 mean temperature to CO₂ emissions. Hence, understanding this high climate sensitiv-
261 ity is most likely key to understanding why some CMIP6 models display such rapid loss
262 of Arctic sea ice. A recent study suggested this high sensitivity to be caused by stronger
263 cloud feedbacks (Zelinka et al., 2020).

264 If we plot the two sensitivity metrics against each other, it is generally impossible
265 to distinguish a given CMIP6 model from the cloud given by CMIP5 models, with the
266 exception of the highly sensitive CMIP6 simulations that clearly fall outside the cloud
267 of previous CMIP phases (Figure 1g). The lack of both such high-sensitive simulations
268 and of very low-sensitive simulations in CMIP5 might be one reason for why the corre-
269 lation between the two metrics is lower for CMIP5 than for CMIP3 and CMIP6.

270 In summary, we find that over the period 1979–2014, CMIP6 models on average
271 simulate a sensitivity of Arctic sea ice that is closer to the observed value than CMIP5
272 and CMIP3 models, both relative to a given CO₂ emission (as a proxy for time) and to
273 a given warming. However, only few models are able to simulate a plausible sea-ice loss
274 sensitivity to cumulative CO₂ emissions and simultaneously a plausible rise in global mean
275 surface temperature.

276 **4 Projections of Future Arctic Sea Ice**

277 The identified spread of CMIP models in simulating the past mean state and sen-
278 sitivity to warming and CO₂ emissions introduces significant model uncertainty into fu-
279 ture projections of the evolution of the Arctic sea-ice cover. This model uncertainty re-
280 mains large in CMIP6.

281 To address this issue when analyzing projections of when Arctic sea-ice area might
282 drop below 1 million km², a commonly used threshold for an ice-free Arctic, we take the
283 following approach. First, we examine the full range of CMIP6 model simulations, not-
284 ing that the model spread provides a wide spectrum of the possible future evolution of
285 Arctic sea-ice area. Second, we narrow the range by considering only those models that
286 have the observations within their ensemble spread simultaneously for two key metrics
287 (compare Massonnet et al., 2012): (a) the 2005–2014 September mean sea-ice area and
288 (b) the observed sensitivity of sea-ice area to cumulative CO₂ emissions over the period
289 1979–2014. We choose these metrics because they correlate with the first sea-ice free year
290 at a correlation of $R > 0.5$ for all scenarios over the entire CMIP6 multi-model ensem-
291 ble. Note, however, that care must be taken when interpreting the range of selected mod-
292 els, as the relationship between past and future evolution of a climate model is not al-
293 ways clear (Jahn et al., 2016; Stroeve & Notz, 2015). On the other hand, it becomes more
294 important that a model plausibly captures the observed mean state of Arctic sea-ice area
295 the lower that mean state becomes, because initial conditions become more important
296 as the observed sea-ice state approaches ice-free conditions and the simulations start en-
297 tering the realm of decadal predictions. We hence trust that the range of uncertainty given
298 by the selected models gives a more realistic estimate of the true model uncertainty than
299 that given by the full CMIP6 multi-model ensemble. The selected models are printed
300 in bold in table S4.

301 In analyzing the future relationship between sea-ice loss and changes in the forc-
302 ing, we find that the simulated correlation between winter Arctic sea-ice area and cu-
303 mulative CO₂ emissions remains high well into the future (Figure 2a). For summer, the
304 linear relationship eventually decreases as more and more years of zero Arctic sea-ice cov-
305 erage are averaged into the multi-model mean (Figure 2d). In interpreting these results
306 quantitatively, it is of course important to note that CO₂, while being the most impor-
307 tant external driver of observed changes in Arctic sea-ice coverage, is not the only cause
308 of observed and future changes. Its dominant role, however, holds well into the future
309 and/or the additional impacts of other anthropogenic forcings, such as methane and aerosols,
310 remain roughly stable over time. Otherwise the correlation between March Arctic sea-
311 ice area and cumulative CO₂ emissions would not remain as stable over time and would
312 not be as independent of the specific forcing scenario (Figure 2a).

313 We also find that the simulated correlation of temperature with winter Arctic sea-
314 ice area remains high well into the future (Figure 2b), while again in summer the cor-
315 relation eventually decreases as more models lose their sea ice completely (Figure 2e).

316 The high correlation between sea-ice loss and changes in the forcing allows us to
317 estimate the cumulative future CO₂ emissions, warming level and eventually year at which
318 the Arctic Ocean will practically be sea-ice free for the first time, defined as the first year
319 in which the monthly mean September sea-ice area drops below 1 million km².

320 We find that CMIP6 models simulate a large spread of cumulative future CO₂ emis-
321 sions at which the Arctic could first become practically sea-ice free in September (Fig-
322 ure 3a). The simulated future emissions for the first occurrence of a practically sea-ice
323 free Arctic Ocean range from 450 Gt CO₂ *below* to more than 5000 Gt CO₂ above present
324 cumulative emissions. However, 158 out of 243 simulations become practically sea-ice
325 free before future cumulative CO₂ emissions reach 1000 GtCO₂ above that of 2019 (equiv-
326 alent to about 3400 GtCO₂ cumulative emissions since 1850). Considering only the mod-
327 els with ensemble members within the plausible range of observed sea-ice evolution, we
328 find a reduced range of 170 Gt below to 2200 Gt above cumulative future anthropogenic
329 CO₂ emissions when Arctic sea-ice area is projected to drop below 1 million km². Of these
330 members from the selected models, the vast majority (101 out of 128) become practi-
331 cally sea-ice free at future cumulative CO₂ emissions less than 1000 Gt. This compares
332 favourably with the range of 800±300 Gt estimated from a direct analysis of the observed

333 sensitivity (Notz & Stroeve, 2018). In combination, these estimates make it appear likely
334 that the Arctic Ocean will practically lose its sea ice cover in September for the first time
335 at future anthropogenic CO₂ emissions of between 200 and 1100 Gt above that of 2019.

336 As a function of GMST, ice-free conditions occur across the entire CMIP6 multi-
337 model ensemble at a global warming of between 0.9 and 3.2 °C above pre-industrial con-
338 ditions of each individual model (Figure 3b). If we select only those models with a rea-
339 sonable simulation of past Arctic sea-ice conditions, the estimated temperature range
340 decreases slightly to 1.3 to 2.9 °C. The upper end of this range is higher than the range
341 of 1.7 ± 0.4 °C estimated from a direct analysis of the observed sensitivity (Notz & Stroeve,
342 2018) and higher than estimates from bias-corrected simulations that all project the first
343 ice-free Arctic at temperatures below 2 °C (Jahn, 2018; Niederdrenk & Notz, 2018; Ri-
344 dley & Blockley, 2018; Screen & Williamson, 2017; Sigmond et al., 2018). This high bias
345 is probably a reflection of the CMIP6 models' weak sensitivity of sea-ice area loss to global
346 warming, resulting in too high estimates of the warming at which the Arctic becomes
347 practically sea-ice free in summer.

348 In the CMIP6 ensemble, the sea-ice area loss per cumulative CO₂ emissions and
349 degree of global warming does barely depend on the forcing scenario (Figure 3a, b). Sce-
350 nario dependence is also very small regarding the near-term future evolution of Arctic
351 summer sea ice as a function of time until about 2040 (Figures 2f and 3c). This is re-
352 lated to the fact that until 2040, the scenarios evolve quite similarly (O'Neill et al., 2016).
353 Furthermore, given that the current sea-ice area is much smaller than it used to be, the
354 importance of internal variability increases relative to the forced change necessary to lose
355 the remaining sea-ice cover in September. As a consequence, for some models the sea
356 ice disappears earlier for the low-emissions scenarios than for the high-emissions scenar-
357 ios in the ensemble members provided to the CMIP6 archive (Table S4). For all scenar-
358 ios, the first year of practically sea-ice-free conditions ranges from some years before present
359 to the end of this century (Table S4), with a clear majority of models reaching ice-free
360 conditions before 2050. This finding remains valid for the selected models. From the mid-
361 dle of the century onward, scenario dependence becomes more and more evident. For ex-
362 ample, the loss of sea-ice area in March occurs much faster from 2050 onward in scenario
363 SSP5-8.5 than in other scenarios (Figure 2c).

5 Conclusion

Based on the analyzed evolution of Arctic sea-ice area and volume in CMIP6 models, in this contribution we have found the following:

- CMIP6 model performance in simulating Arctic sea ice is similar to CMIP3 and CMIP5 model performance in many aspects. This includes models simulating a wide spread of mean sea-ice area and volume in March and September; the multi-model ensemble spread capturing the observed mean sea-ice area in March and September; the models' general underestimation of the sensitivity of September sea-ice area to a given amount of global warming; as well as most models' failure to simulate at the same time a plausible evolution of sea-ice area and of global mean surface temperature.
- CMIP6 model performance differs from CMIP3 and CMIP5 in some aspects. These include a larger fraction of CMIP6 models capturing the observed sensitivity of Arctic sea ice to anthropogenic CO₂ emissions and the CMIP6 multi-model ensemble mean being closer to the observed sensitivity of Arctic sea ice to global warming. It is unclear to what degree these improvements are caused by a change in the forcing versus improvement of model physics.
- The CMIP6 models simulate a large spread for when Arctic sea-ice area is predicted to drop below 1 million km², such that the Arctic Ocean becomes practically sea-ice free. However, the clear majority of all models, and of those models that best capture the observed evolution, project that the Arctic will become practically sea-ice free in September before the year 2050 at future anthropogenic CO₂ emissions of less than 1000 GtCO₂ above that of 2019 in all scenarios.

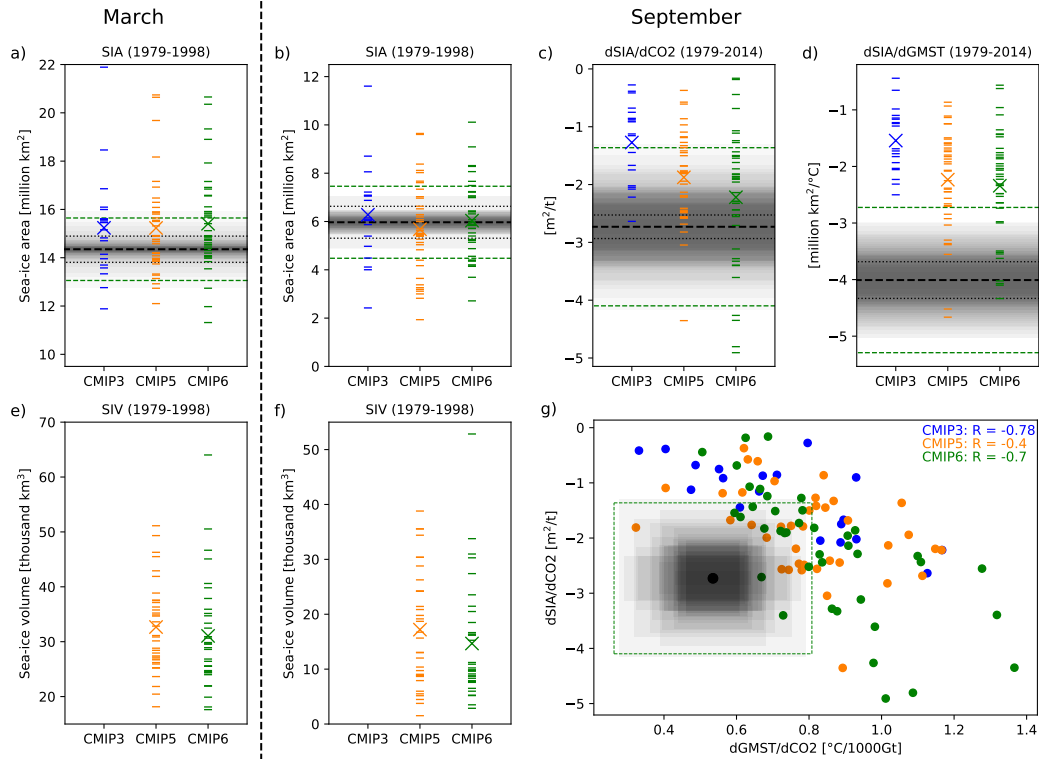
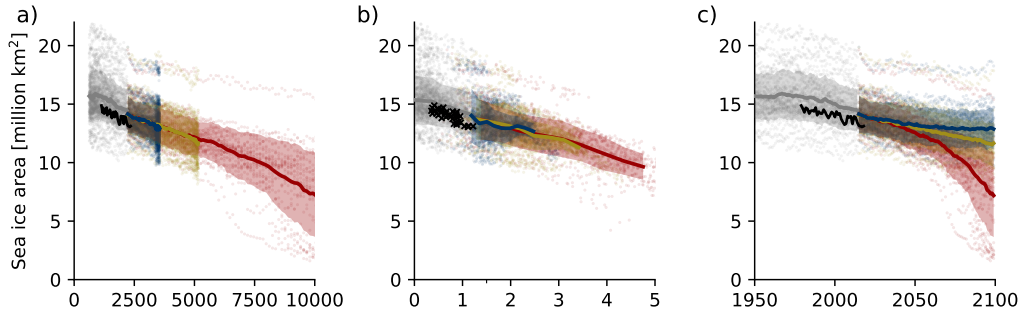


Figure 1. Comparison of sea-ice metrics as simulated by the first ensemble members of CMIP3 (blue), CMIP5 (orange) and CMIP6 (green) models. The individual panels show the mean Arctic sea-ice area (SIA) in (a) March and (b) September for 1979–1998; mean Arctic sea-ice volume (SIV) in (e) March and (f) September for 1979–1998; and (c-d) the sensitivity over the period 1979–2014 of September sea-ice area to (c) CO₂ emissions and (d) global annual mean surface temperature (GMST). (g) The sensitivity of Arctic sea-ice area to CO₂ emissions scattered against the sensitivity of GMST to CO₂ emissions. In (a-f), horizontal dashes represent the first ensemble member of each model and crosses represent the multi-model ensemble mean. The thick dashed black lines denote the average of the observational satellite products, where available. The dotted lines denote one standard deviation of observational uncertainty. The green dashed lines denote the 2 σ plausible range including internal variability and observational uncertainty as defined in section 2. The gray shadings around the lines denote overlays of estimated internal variability from all CMIP6 models with three or more ensemble members, with each overlay representing the 1-standard-deviation spread of a single model. Hence, the darker the shading, the more models agree on internal variability to cover a certain range.

Article
 Accepted

March



September

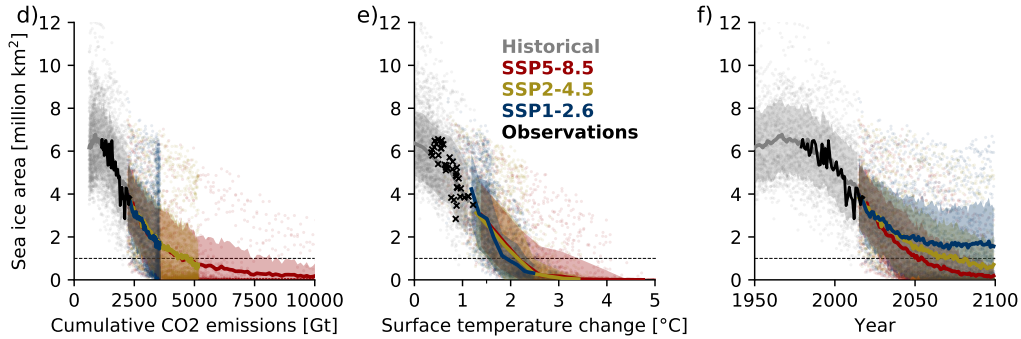


Figure 2. Evolution of Arctic sea-ice area over the historical period and following three scenario projections in (a-c) March and (d-f) September as a function of (a,d) cumulative anthropogenic CO₂ emissions, (b,e) global annual mean surface temperature anomaly and (c,f) time for all available CMIP6 models. Thick lines denote the multi-model ensemble mean, where all models are represented by their first ensemble member, and the shading around the lines indicates one standard deviation around the multi-model mean. Faint dots denote the first ensemble member of each model and thick black lines and crosses denote observations. Note that discontinuities in the multi-model ensemble mean arise from a different number of available models for the historical period and the scenario simulations.

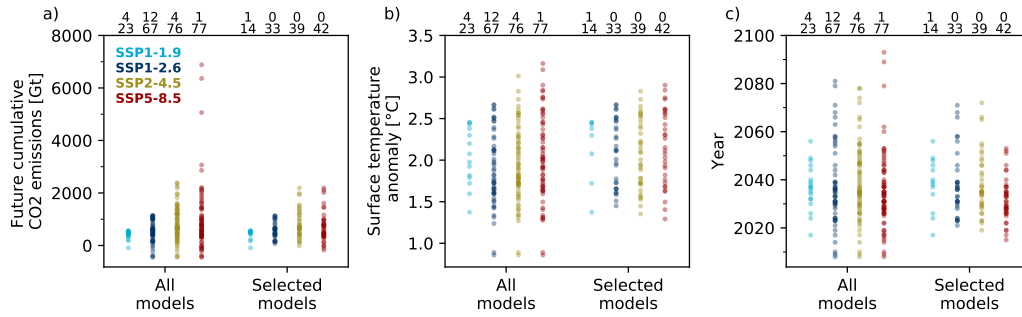


Figure 3. CMIP6 projections of (a) future cumulative CO₂ emissions, (b) global annual mean surface temperature anomaly and (c) year when September-mean sea-ice area drops below 1 million km² for the first time in each simulation. The numbers at the top of the panels denote the number of simulations that do not simulate a sea-ice cover below 1 million km² by 2100 (top row) and the total number of simulations (bottom row) for each scenario. Each dot represents a single simulation, with all available CMIP6 simulations shown in the figure.

387 **Appendix A Authors**

388 All authors contributed to discussions and the writing of the paper, as well as im-
389 plementation or analysis of SIMIP variables in CMIP6 models. Additional contributions
390 are listed below.

391 Dirk Notz, Center for Earth System Research and Sustainability (CEN), Univer-
392 sity of Hamburg and Max Planck Institute for Meteorology, Hamburg, Germany; co-chair
393 of SIMIP, lead the development of this paper, contributed to implementing the SIMIP
394 protocol in MPI-ESM

395 Jakob Dörr, Max Planck Institute for Meteorology, Hamburg, Germany; carried
396 out all data analysis for this paper; compiled all figures and tables

397 David A Bailey, Climate and Global Dynamics Laboratory, National Center for At-
398 mospheric Research, Boulder, Colorado, United States of America

399 Ed Blockley, Met Office Hadley Centre, Exeter, United Kingdom ; contributed to
400 the sea ice component of the UKESM and HadGEM3 models

401 Mitchell Bushuk, Geophysical Fluid Dynamics Laboratory, Princeton, New Jersey,
402 United States of America

403 Jens Boldingh Debernard, Norwegian Meteorological Institute, Norway; contribu-
404 tion to the sea ice component of NorESM2-LM

405 Evelien Dekker, Rossby Centre, Swedish Meteorological and Hydrological Institute,
406 Norrköping, Meteorological Department at Stockholm University, Sweden

407 Patricia DeRepentigny, Department of Atmospheric and Oceanic Sciences and In-
408 stitute of Arctic and Alpine Research, University of Colorado Boulder, Boulder, Colorado,
409 United States of America

410 David Docquier, Rossby Centre, Swedish Meteorological and Hydrological Insti-
411 tute, Norrköping, Sweden

412 Neven S. Fućkar, Environmental Change Institute, University of Oxford, Oxford,
413 UK, and Earth Sciences Department, Barcelona Supercomputing Center, Barcelona, Spain

414 John C. Fyfe, Canadian Centre for Climate Modelling and Analysis, Environment
415 and Climate Change Canada

416 Alexandra Jahn, University of Colorado Boulder, Department of Atmospheric and
417 Oceanic Sciences and Institute of Arctic and Alpine Research, Boulder, Colorado, United
418 States of America; co-chair of SIMIP

419 Marika Holland, Climate and Global Dynamics Laboratory, National Center for
420 Atmospheric Research, Boulder, Colorado, United States of America; SIMIP steering-
421 group member

422 Elizabeth Hunke, Theoretical Division, Los Alamos National Laboratory, Los Alamos,
423 New Mexico, United States of America; SIMIP steering-group member

424 Dorothea Iovino, Ocean Modeling and Data Assimilation Division, Centro Euro-
425 Mediterraneo sui Cambiamenti Climatici, Italy

426 Narges Khosravi, Alfred Wegener Institute, Helmholtz Centre for Polar and Ma-
427 rine Research, Bremerhaven, Germany

428 Gurvan Madec, Sorbonne Universits, UPMC Paris 6, LOCEAN-IPSL, CNRS/IRD/MNHN,
429 Paris, France

430 François Massonnet, Georges Lematre Centre for Earth and Climate Research, Earth
431 and Life Institute, Universit catholique de Louvain, Louvain-la-Neuve, Belgium; SIMIP
432 steering-group member

433 Siobhan O'Farrell, CSIRO Oceans and Atmosphere, Aspendale, Victoria, Australia

434 Alek Petty, Cryospheric Sciences Laboratory, NASA Goddard Space Flight Cen-
435 ter, Greenbelt, Maryland, United States of America, and Earth System Science Inter-
436 disciplinary Center, University of Maryland, College Park, Maryland, United States of
437 America

438 Arun Rana, Georges Lematre Centre for Earth and Climate Research, Earth and
439 Life Institute, Universit catholique de Louvain, Louvain-la-Neuve, Belgium

440 Lettie Roach, Atmospheric Sciences, University of Washington, Seattle, Washing-
441 ton, United States of America

442 Erica Rosenblum, Centre for Earth Observation Science, University of Manitoba,
443 Winnipeg, Manitoba, Canada; contributed to the preliminary data analysis

444 Clement Rousset, Sorbonne Universits, UPMC Paris 6, LOCEAN-IPSL, CNRS/IRD/MNHN,
445 Paris, France

446 Tido Semmler, Alfred Wegener Institute, Helmholtz Centre for Polar and Marine
447 Research, Bremerhaven, Germany

448 Julienne Stroeve, University College London, London, United Kingdom and Na-
449 tional Snow and Ice Data Center, Boulder, Colorado, United States of America; SIMIP
450 steering-group member

451 Takahiro Toyoda, Meteorological Research Institute, Japan Meteorological Agency,
452 Japan; contributed to carry out the MRI-ESM2 experiments and to prepare the output
453 for SIMIP analyses

454 Bruno Tremblay, Department of Atmospheric and Oceanic Sciences, McGill Uni-
455 versity, Montreal, Canada; SIMIP steering-group member.

456 Hiroyuki Tsujino, Meteorological Research Institute, Japan Meteorological Agency,
457 Japan; contributed to carry out the MRI-ESM2 experiments and to prepare the output
458 for SIMIP analyses

459 Martin Vancoppenolle, Sorbonne Universits, UPMC Paris 6, LOCEAN-IPSL, CNRS/
460 IRD/ MNHN, Paris, France; SIMIP steering-group member; contributed to the sea ice
461 component of IPSL-CM and EC-Earth

462 **Acknowledgments**

463 We thank two anonymous reviewers for their valuable feedback that helped improving
464 this manuscript.

465 We are grateful to all modeling centers for carrying out CMIP6 simulations used
466 here. The data used for this study are freely available from the Earth System Grid Fed-
467 eration (ESGF) at esgf-node.llnl.gov/search/cmip6. See supporting information for
468 a detailed listing of all CMIP6 data sets used in this study, including their dois. The scripts
469 for analysis and plotting of the data are available from [https://github.com/jakobdoerr/](https://github.com/jakobdoerr/SIMIP_2020)
470 [SIMIP_2020](https://github.com/jakobdoerr/SIMIP_2020).

471 EC-Eart3-Veg simulations that are not published on ESGF yet are locally stored
472 at the Swedish Meteorological and Hydrological Institute (cmip6-data@ecearth.org). We

473 thank the EC-Earth consortium that realized the development of EC-Earth. The EC-
474 Earth3-Veg simulations were done as part of the European Union's Horizon 2020 research
475 and innovation programme under grant agreement No 641816 (CRESCENDO) on re-
476 sources provided by the Swedish National Infrastructure for Computing (SNIC) at PDC
477 and NSC.

478 Previous and current CESM versions are freely available at www.cesm.ucar.edu/models.
479 The CESM project is supported primarily by the National Science Foundation (NSF).
480 This material is based upon work supported by the National Center for Atmospheric Re-
481 search, which is a major facility sponsored by the NSF under Cooperative Agreement
482 No. 1852977. Computing and data storage resources, including the Cheyenne supercom-
483 puter (doi:10.5065/D6RX99HX), were provided by the Computational and Information
484 Systems Laboratory (CISL) at NCAR. We thank all the scientists, software engineers,
485 and administrators who contributed to the development of CESM2.

486 The ACCESS-CM2 CMIP6 submission was jointly funded through CSIRO and the
487 Earth Systems and Climate Change Hub of the Australian Government's National En-
488 vironmental Science Program, with support from the Australian Research Council Cen-
489 tre of Excellence for Climate System Science. The ACCESS-ESM1.5 CMIP6 submission
490 was supported by the CSIRO Climate Science Centre.

491 Parts of the work described in this paper has received funding from the European
492 Union's Horizon 2020 Research and Innovation programme through grant agreement No.
493 727862 APPLICATE. The content of the paper is the sole responsibility of the authors
494 and it does not represent the opinion of the European Commission, and the Commis-
495 sion is not responsible for any use that might be made of information contained.

496 We thank the WCRP-CliC Project for supporting the SIMIP project.

497 E. Blockley was supported by the Joint UK BEIS/Defra Met Office Hadley Cen-
498 tre Climate Programme (GA01101)

499 J. B. Debernard is supported by the Research Concile of Norway through INES (270061).

500 E. Dekker is supported by the Arctic Across Scales Project through the Knut and
501 Alice Wallenberg Foundation (KAW2016.0024)

502 P. DeRepentigny is supported by the Natural Sciences and Engineering Council of
503 Canada, the Fond de recherche du Quebec – Nature et Technologies and the Canadian
504 Meteorological and Oceanographic Society through PhD scholarships and NSF-OPP award
505 1847398.

506 D. Docquier is funded by the EU Horizon 2020 OSeaIce project, under the Marie
507 Sklodowska-Curie grant agreement no. 834493.

508 J. Dörr is funded by the German Ministry for Education and Research through the
509 project “Meereis bei +1.5 °C”.

510 N.S. Fučkar acknowledges support of H2020 MSCA IF (Grant ID 846824).

511 E. Hunke is supported by the Regional and Global Modeling and Analysis program
512 of the Department of Energy’s Biological and Environmental Research division.

513 A. Jahn’s contribution is supported by NSF-OPP award 1847398.

514 F. Massonnet is a F.R.S.-FNRS Research Fellow.

515 D. Notz is funded by the Deutsche Forschungsgemeinschaft under Germanys Ex-
516 cellence Strategy EXC 2037 ‘CLICCS - Climate, Climatic Change, and Society’ Project
517 Number: 390683824, contribution to the Center for Earth System Research and Sustain-
518 ability (CEN) of Universität Hamburg.

519 L. Roach was supported by the National Science Foundation grant PLR-1643431
520 and National Oceanic and Atmospheric Administration grant NA18OAR4310274.

521 J. Stroeve and E. Rosenblum are supported by the Canada C150 Chair Program

522 This work is a contribution to NSF-OPP award 1504023 awarded to B. Tremblay.

523 **References**

524 Bunzel, F., Notz, D., & Pedersen, L. T. (2018). Retrievals of Arctic Sea-Ice Volume
525 and Its Trend Significantly Affected by Interannual Snow Variability. *Geophys-*
526 *ical Research Letters*, *45*(21), 11,751–11,759. doi: 10.1029/2018GL078867

527 Cavalieri, D. J., Parkinson, C. L., Gloersen, P., & Zwally, H. J. (1997). *Arctic and*
528 *Antarctic Sea Ice Concentrations from Multichannel Passive-microwave Satel-*
529 *lite Data Sets: October 1978 to December 1996* (Technical Memorandum No.

- 530 104647). NASA.
- 531 Checa-Garcia, R., Hegglin, M. I., Kinnison, D., Plummer, D. A., & Shine, K. P.
532 (2018). Historical tropospheric and stratospheric ozone radiative forcing using
533 the CMIP6 database. *Geophysical Research Letters*, *45*(7), 3264–3273. doi:
534 10.1002/2017GL076770
- 535 Chevallier, M., Smith, G. C., Dupont, F., Lemieux, J.-F., Forget, G., Fujii, Y.,
536 ... Wang, X. (2017). Intercomparison of the Arctic sea ice cover in global
537 oceansea ice reanalyses from the ORA-IP project. *Clim. Dynam.*, *49*(3),
538 1107–1136. doi: 10.1007/s00382-016-2985-y
- 539 Comiso, J. C., Cavalieri, D. J., Parkinson, C. L., & Gloersen, P. (1997). Passive mi-
540 crowave algorithms for sea ice concentration: A comparison of two techniques.
541 *Remote Sens. Env.*, *60*(3), 357–384. doi: 10.1016/S0034-4257(96)00220-9
- 542 Comiso, J. C., Meier, W. N., & Gersten, R. (2017). Variability and trends in the
543 Arctic sea ice cover: Results from different techniques. *Journal of Geophysical*
544 *Research: Oceans*, *122*(8), 6883–6900.
- 545 England, M., Jahn, A., & Polvani, L. (2019). Nonuniform contribution of internal
546 variability to recent Arctic sea ice loss. *J. Climate*, *32*(13), 4039–4053. doi: 10
547 .1175/JCLI-D-18-0864.1
- 548 Eyring, V., Bony, S., Meehl, G. A., Senior, C., Stevens, B., Stouffer, R. J., & Taylor,
549 K. E. (2015). Overview of the Coupled Model Intercomparison Project Phase
550 6 (CMIP6) experimental design and organisation. *Geosci. Model Dev. Discuss.*,
551 *8*(12), 10539–10583. doi: 10.5194/gmdd-8-10539-2015
- 552 Gidden, M., Riahi, K., Smith, S., Fujimori, S., Luderer, G., Kriegler, E., ... others
553 (2019). Global emissions pathways under different socioeconomic scenarios
554 for use in CMIP6: a dataset of harmonized emissions trajectories through the
555 end of the century. *Geoscientific model development*, *12*(4), 1443–1475. doi:
556 10.5194/gmd-12-1443-2019
- 557 GISTEMP Team. (2019). *GISS Surface Temperature Analysis (GISTEMP), version*
558 *4*. NASA Goddard Institute for Space Studies [date accessed: XX/XX/XX].
559 Retrieved from <https://data.giss.nasa.gov/gistemp/>
- 560 Global Carbon Project. (2019). *Supplemental data of global carbon budget 2019 (ver-*
561 *sion 1.0 [data set]*. doi: doi.org/10.18160/gcp-2019
- 562 Gregory, J. M., Stott, P. A., Cresswell, D. J., Rayner, N. A., Gordon, C., & Sex-

- 563 ton, D. M. H. (2002). Recent and future changes in Arctic sea ice sim-
 564 ulated by the HadCM3 AOGCM. *Geophys. Res. Lett.*, *29*(24), 2175,
 565 doi:10.1029/2001GL014575.
- 566 Herrington, T., & Zickfeld, K. (2014). Path independence of climate and carbon
 567 cycle response over a broad range of cumulative carbon emissions. *Earth Syst.*
 568 *Dynam.*, *5*, 409422. doi: 10.5194/esd-5-409-2014
- 569 Jahn, A. (2018). Reduced probability of ice-free summers for 1.5 °C compared to 2
 570 °C warming. *Nat. Clim. Change*. doi: 10.1038/s41558-018-0127-8
- 571 Jahn, A., Kay, J. E., Holland, M. M., & Hall, D. M. (2016). How predictable is the
 572 timing of a summer ice-free Arctic? *Geophys. Res. Lett.*, 2016GL070067. doi:
 573 10.1002/2016GL070067
- 574 Kay, J. E., Holland, M. M., & Jahn, A. (2011). Inter-annual to multi-decadal Arc-
 575 tic sea ice extent trends in a warming world. *Geophys. Res. Lett.*, *38*. doi: 10
 576 .1029/2011GL048008
- 577 Koenigk, T., Devasthale, A., & Karlsson, K.-G. (2014). Summer Arctic sea ice
 578 albedo in CMIP5 models. *Atmos. Chem. Phys.*, *14*(4), 1987–1998. doi: 10
 579 .5194/acp-14-1987-2014
- 580 Lavergne, T., Srensen, A. M., Kern, S., Tonboe, R., Notz, D., Aaboe, S., ... Ped-
 581 ersen, L. T. (2019). Version 2 of the EUMETSAT OSI SAF and ESA CCI
 582 sea-ice concentration climate data records. *The Cryosphere*, *13*(1), 49–78. doi:
 583 https://doi.org/10.5194/tc-13-49-2019
- 584 Lenssen, N. J., Schmidt, G. A., Hansen, J. E., Menne, M. J., Persin, A., Ruedy,
 585 R., & Zyss, D. (2019). Improvements in the GISTEMP uncertainty model.
 586 *Journal of Geophysical Research: Atmospheres*, *124*(12), 6307–6326. doi:
 587 10.1029/2018JD029522
- 588 Mahlstein, I., & Knutti, R. (2012). September Arctic sea ice predicted to disappear
 589 near 2 °C global warming above present. *J. Geophys. Res.*, *117*, D06104. doi:
 590 10.1029/2011JD016709
- 591 Massonnet, F., Fichet, T., Goosse, H., Bitz, C. M., Philippon-Berthier, G., Hol-
 592 land, M. M., & Barriat, P.-Y. (2012). Constraining projections of summer
 593 Arctic sea ice. *The Cryosphere*, *6*(6), 1383–1394. doi: 10.5194/tc-6-1383-2012
- 594 Melia, N., Haines, K., & Hawkins, E. (2015). Improved Arctic sea ice thickness pro-
 595 jections using bias-corrected CMIP5 simulations. *The Cryosphere*, *9*(6), 2237–

- 596 2251. doi: 10.5194/tc-9-2237-2015
- 597 Morice, C. P., Kennedy, J. J., Rayner, N. A., & Jones, P. D. (2012). Quantifying
598 uncertainties in global and regional temperature change using an ensemble of
599 observational estimates: The HadCRUT4 data set. *Journal of Geophysical
600 Research Atmospheres*, *117*(8), 1–22. doi: 10.1029/2011JD017187
- 601 Niederdrenk, A. L., & Notz, D. (2018). Arctic Sea Ice in a 1.5°C Warmer World.
602 *Geophys. Res. Lett.*, *45*(4), 1963–1971. doi: 10.1002/2017GL076159
- 603 Notz, D. (2014). Sea-ice extent and its trend provide limited metrics of model per-
604 formance. *The Cryosphere*, *8*(1), 229–243. doi: 10.5194/tc-8-229-2014
- 605 Notz, D. (2015). How well must climate models agree with observations? *Phil.
606 Trans. R. Soc. A*, *373*(2052), 20140164. doi: 10.1098/rsta.2014.0164
- 607 Notz, D., Jahn, A., Holland, M., Hunke, E., Massonnet, F., Stroeve, J., ... Van-
608 coppenolle, M. (2016). Sea Ice Model Intercomparison Project (SIMIP):
609 Understanding sea ice through climate-model simulations. *Geoscientific Model
610 Development Discussions*, 1–29. doi: 10.5194/gmd-2016-67
- 611 Notz, D., & Stroeve, J. (2016). Observed Arctic sea-ice loss directly follows anthro-
612 pogenic CO₂ emission. *Science*, aag2345. doi: 10.1126/science.aag2345
- 613 Notz, D., & Stroeve, J. (2018). The trajectory towards a seasonally ice-free Arctic
614 Ocean. *Current Climate Change Reports*, *4*(4), 407–416. doi: 10.1007/s40641
615 -018-0113-2
- 616 Olason, E., & Notz, D. (2014). Drivers of variability in Arctic sea-ice drift speed.
617 *Journal of Geophysical Research: Oceans*, *119*(9), 5755–5775.
- 618 Olonscheck, D., & Notz, D. (2017). Consistently Estimating Internal Climate Vari-
619 ability from Climate Model Simulations. *J. Clim.*, *30*(23), 9555–9573. doi: 10
620 .1175/JCLI-D-16-0428.1
- 621 O’Neill, B. C., Tebaldi, C., Van Vuuren, D. P., Eyring, V., Friedlingstein, P., Hurtt,
622 G., ... Sanderson, B. M. (2016). The Scenario Model Intercomparison Project
623 (ScenarioMIP) for CMIP6. *Geoscientific Model Development*, *9*(9), 3461–3482.
624 doi: 10.5194/gmd-9-3461-2016
- 625 Riahi, K., van Vuuren, D. P., Kriegler, E., Edmonds, J., O’Neill, B. C., Fujimori, S.,
626 ... Tavoni, M. (2017). The shared socioeconomic pathways and their energy,
627 land use, and greenhouse gas emissions implications: An overview. *Global
628 Environmental Change*, *42*, 153 - 168. doi: 10.1016/j.gloenvcha.2016.05.009

- 629 Ridley, J., & Blockley, E. (2018). Solar radiation management not as effective as
 630 CO₂ mitigation for Arctic sea ice loss in hitting the 1.5 and 2 °C COP climate
 631 targets. *The Cryosphere*(12), 3355–3360. doi: 10.5194/tc-12-3355-2018
- 632 Roach, L. A., Dörr, J., Holmes, C. R., Massonnet, F., Blockley, E. W., Notz, D.,
 633 ... Bitz, C. M. (2020). Antarctic sea ice in CMIP6. *Geophys. Res. Lett.*,
 634 2019GL086729.
- 635 Rohde, R., Muller, R., Jacobsen, R., Perlmutter, S., & Mosher, S. (2013). Berke-
 636 ley Earth Temperature Averaging Process. *Geoinformatics & Geostatistics: An*
 637 *Overview*, 01(02). doi: 10.4172/2327-4581.1000103
- 638 Rosenblum, E., & Eisenman, I. (2016). Faster Arctic sea ice retreat in CMIP5 than
 639 in CMIP3 due to volcanoes. *J. Climate*, 29(24), 9179–9188. doi: 10.1175/JCLI
 640 -D-16-0391.1
- 641 Rosenblum, E., & Eisenman, I. (2017). Sea Ice Trends in Climate Models Only Ac-
 642 curate in Runs with Biased Global Warming. *J. Clim.*, 30(16), 6265–6278. doi:
 643 10.1175/JCLI-D-16-0455.1
- 644 Screen, J. A., & Williamson, D. (2017). Ice-free Arctic at 1.5 °C? *Nat. Clim.*
 645 *Change*, 7(4), 230–231. doi: 10.1038/nclimate3248
- 646 Shu, Q., Song, Z., & Qiao, F. (2015). Assessment of sea ice simulations in the
 647 CMIP5 models. *The Cryosphere*, 9(1), 399–409. doi: 10.5194/tc-9-399-2015
- 648 Sigmond, M., Fyfe, J. C., & Swart, N. C. (2018). Ice-free Arctic projections under
 649 the Paris Agreement. *Nat. Clim. Change*. doi: 10.1038/s41558-018-0124-y
- 650 Stroeve, J., Barrett, A., Serreze, M., & Schweiger, A. (2014). Using records
 651 from submarine, aircraft and satellites to evaluate climate model simula-
 652 tions of Arctic sea ice thickness. *The Cryosphere*, 8(5), 1839–1854. doi:
 653 10.5194/tc-8-1839-2014
- 654 Stroeve, J., Holland, M. M., Meier, W., Scambos, T., & Serreze, M. (2007). Arc-
 655 tic sea ice decline: Faster than forecast. *Geophys. Res. Lett.*, 34, L09501,
 656 doi:10.1029/2007GL029703.
- 657 Stroeve, J., Kattsov, V., Barrett, A., Serreze, M., Pavlova, T., Holland, M., & Meier,
 658 W. N. (2012). Trends in Arctic sea ice extent from CMIP5, CMIP3 and obser-
 659 vations. *Geophys. Res. Lett.*, 39(16), L16502. doi: 10.1029/2012GL052676
- 660 Stroeve, J., & Notz, D. (2015). Insights on past and future sea-ice evolution from
 661 combining observations and models. *Glob. Planet Change*, 135, 119–132. doi:

- 662 10.1016/j.gloplacha.2015.10.011
- 663 Swart, N. C., Fyfe, J. C., Hawkins, E., Kay, J. E., & Jahn, A. (2015). Influence of
664 internal variability on Arctic sea-ice trends. *Nat. Clim. Change*, *5*(2), 86–89.
665 doi: 10.1038/nclimate2483
- 666 Vose, R. S., Arndt, D., Banzon, V. F., Easterling, D. R., Gleason, B., Huang, B.,
667 ... Wuertz, D. B. (2012). NOAA’s merged land-ocean surface temperature
668 analysis. *Bulletin of the American Meteorological Society*, *93*(11), 1677–1685.
669 doi: 10.1175/BAMS-D-11-00241.1
- 670 Winton, M. (2011). Do Climate Models Underestimate the Sensitivity of Northern
671 Hemisphere Sea Ice Cover? *J. Clim.*, *24*(15), 3924–3934.
- 672 Zelinka, M. D., Myers, T. A., McCoy, D. T., Po-Chedley, S., Caldwell, P. M.,
673 Ceppi, P., ... Taylor, K. E. (2020). Causes of higher climate sensitivity in
674 cmip6 models. *Geophysical Research Letters*, *47*(1), e2019GL085782. doi:
675 10.1029/2019GL085782
- 676 Zickfeld, K., Arora, V. K., & Gillett, N. P. (2012). Is the climate response to CO₂
677 emissions path dependent? *Geophys. Res. Lett.*, *39*, L05703. doi: 10.1029/
678 2011GL050205
- 679 Zygmontowska, M., Rampal, P., Ivanova, N., & Smedsrud, L. H. (2014). Uncertain-
680 ties in Arctic sea ice thickness and volume: new estimates and implications for
681 trends. *The Cryosphere*, *8*(2), 705–720. doi: 10.5194/tc-8-705-2014